Weather Radar Rainfall Summer Analysis of Irrigated vs Rainfed Nearby Areas

Author: FRANCESC POLLS I AGELL
Supervisor: JOAN BECH, joan.bech@ub.edu
Facultat de Física, Universitat de Barcelona, Martí i Franquès 1, 08028 Barcelona, Spain*.

Abstract: The objective of this work is to study rainfall characteristics (frequency, amount and type) in a semi-arid region in the Eastern Ebro basin (Iberian Peninsula). The region is included approximately in a 20 km per 30 km rectangle and is divided in two different areas, one irrigated with an artificial channel, and another one non-irrigated. The two areas may present a big difference of surface temperature in a short distance, particularly during midday hours of summer months due to high evapotranspiration contrasts. The study focusses in finding possible differences in rainfall characteristics between two areas. The methodology used is based on the analysis of radar reflectivity data, which is processed to determine the rainfall type, classified in convective and non-convective, a part of rain occurrence and amount. The work examined June, July and August data from years 2014 to 2020 analysing daily, monthly and total rain events distributions in both areas. The results show a big variability of the rainfall in the region depending on the year and as expected, an increase in convective rain in both areas during the afternoon. Although there is not a significant difference in the rainfall type nor in the convective rainfall rate between areas, there is a difference in the convective rain distribution along each area, being the rain in the irrigated part less homogenous than the non-irrigated part. This study has been performed in the framework of the Analysis of Precipitation Processes in the Eastern Ebro Subbasin project (WISE-PreP, RTI2018-098693-B-C32/AEI).

I. INTRODUCTION

Rain is defined as “Precipitation in the form of liquid water drops that have diameters greater than 0.5 mm, or, if widely scattered, the drops may be smaller” (AMS, 2021). Rain can be classified according to characteristics such as, the thermodynamic phase of the water, the rainfall rate, or the rain regime, among others. Rain regime classification will be the focus of our study.

Basically, there are two types of rain: Convective and Stratiform Rain, and sometimes intermediate types. We will simplify the classification as Convective or Non-Convective Rainfall. The Glossary of Meteorology of the AMS, describe Convective Rainfall as “precipitation particles forming in the active updraft of a cumulonimbus cloud, growing primarily by the collection of cloud droplets (i.e., by coalescence and /or riming) and falling out not far from their originating updraft” (AMS, 2021) . On the other hand, the AMS describe Stratiform rain as a “region of precipitation from a nimbostratus cloud, which may or may not be an outgrowth of a cumulonimbus cloud, in which the air motions are strong enough for vapor to be condensed or deposited on particles but weak enough that the particles cannot grow effectively by collection of cloud water droplets”.

Other articles describe stratiform rain according to the characterization of the vertical motion (Houze, 1997), the drop size and the velocity fall using a disdrometer (Thurai et al., 2016) or evaluating the top of the rain clouds.

Another difference between the Convective and Stratiform rain is the rainfall rate. In the first case it is far more intense than in the Stratiform regime. That means that we could evaluate the rain type measuring the rainfall rate in short periods of time using a rain gauge (Llasat, 2001). And of course, if we could affirm that the Convective Rain has a higher rainfall rate vs the stratiform rain it means that we can classify it with the reflectivity data from a meteorological radar.

A conventional scanning meteorological radar provide us the reflectivity precipitation of an extended area. That is the most important difference compared to other instruments like a rain gauge or a disdrometer, which both only can give us point *in situ* measurements. Moreover, a scanning radar could provide the reflectivity characteristics of a big area in 2d or 3d grid. But, of course, the data would not have the same accuracy as the disdrometer or rain gauge.

The main objective of this work is to study the type of rain in a specific area of Catalonia. This study is performed in the framework of the LIAISE program, in particular within the WISE-PreP (Analysis of Precipitation Processes in the Eastern Ebro Subbasin Project). The region of study, as will be described later, has special different characteristics in a small area that could create local differences: it has a clearly irrigated area, and a dry non-irrigated area, side by side. Recently other studies in the same region have analyzed the precipitation using the data from the Weather Radar Network (XRAD) (Roura, 2020) and found that some differences of the accumulated rainfall inside this area could exist.

II. METHODOLOGY

The methodology to perform the classification of the rain type is based on the analysis of the radar reflectivity from a Constant Plan Position Indicator (CAPPI) product (Fabry, 2015). Once classified, the rainfall type will be evaluated to study the diurnal cycle, the summer monthly distribution, and its characterization in each one of the areas.

A. Region of study

The LIAISE project (Land surface Interactions with the Atmosphere over the Iberian Semi-arid Environment) (Boone et al., 2019) perform in the context of the HyMex Programme (Drobinski et al., 2014) studies the possible affectation that human activity can produce to the water cycle. In this project the area of study is situated in the region of Eastern Ebro basin Ebro. This region is one of the driest places in Catalonia, with a semiarid climate. There is an artificial channel that brings water from the Segre River and divides this area in two different parts, an irrigated area (West area) with lots of agriculture fields, and a non-irrigated area (East area) with the intrinsic characteristics of the region and rain-fed fields (see **Figure 1**). The whole region of study is approximately a rectangle of 20-30 km. The two West and East areas do not have the same extension, but both can be considered flat, and consequently, the orography of the terrain does not affect the local meteorological conditions.

From a climatological point of view this region is classified as a Mediterranean Continental Dry area according to Meteocat (*SMC*, 2021). It has a historical climatology of 14 days of rain during the summer season (June, July and

* Electronic address: frpollsa7@alumnes.ub.edu

August) with 70 mm during all the summer (data collected by the AEMET Meteorological Station from Lleida 1971-2001).

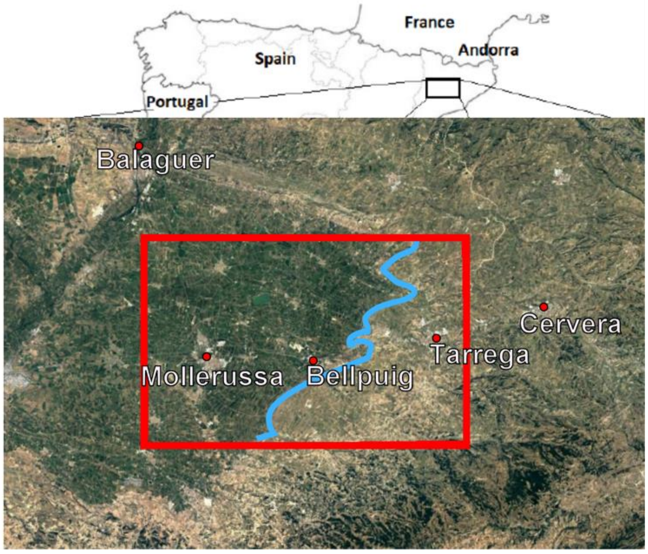

Figure 1: Google Earth image showing the region of study (red rectangle), the channel dividing the two areas (blue line) and some of the principal towns.

Another characteristic of the area of study, and one of the properties that motivates the investigation of the region, is the difference of the surface temperatures. In the MODIS image in **Figure 2** it is clearly seen that there is a difference of almost 10 K of temperature between the irrigated area and the non-irrigated area. The reason is the higher evapotranspiration (sun of water evaporation and plant transpiration) of the irrigated area compared to the non-irrigated area. This contrast between the irrigated and non-irrigated areas is maximum during the summer months. For this reason, the study is focused on the months of June, July and August.

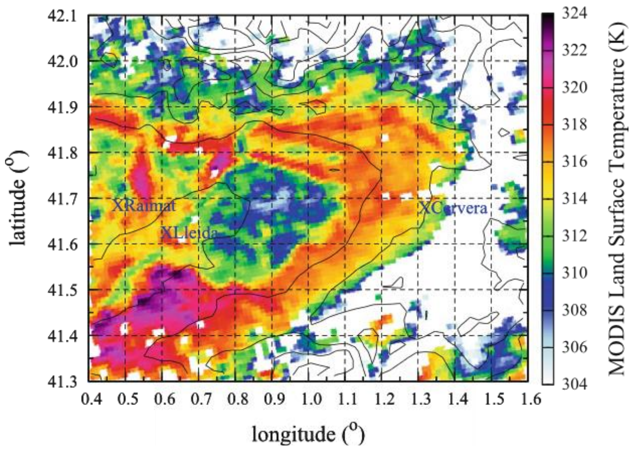

Figure 2. Land surface temperature obtained from MODIS during 5 July 2009 at 13 h UTC in the area of study between Cervera and Lleida (Indicated in the map). White areas indicate no data. (Cuxart et al., 2012).

Another previous study regarding storm initiation (Rigo et al., 2008) showed interesting differences in these two areas and partly motivated the analysis of the local precipitation characteristics (**Figure 3**). In particular there is a local minimum in the number of starting storms (about 0) in the East area and a local maximum (about 3) in the West part.

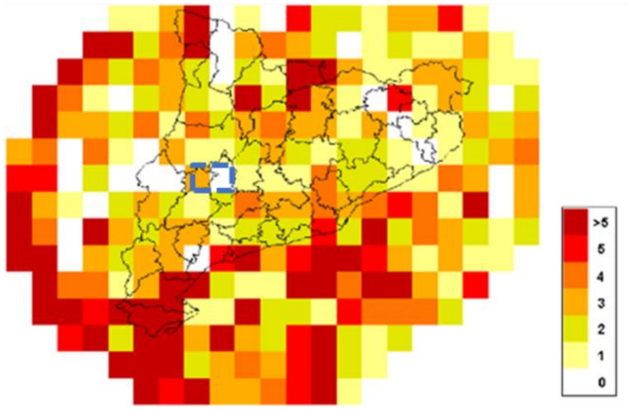

Figure 3. Storm initiation spatial distribution from 2004 to 2006. The blue square indicates the area of study Rigo et al. (2008).

B. Datasets

The data used in this study were recorded with the Meteorological Service of Catalonia C-band weather radar network (Bech et al., 2005). They consist in Geo-TIF files with CAPPI 3d grid radar reflectivity with 10 vertical levels separated each 1 km. This reflectivity data has a spatial and temporal resolution of 2 km x 2km and 6 minutes, respectively.

The first idea was to analyse the reflectivity of all the days and all times during the summer months (June, July and August) from 2014 to 2020. That means 240 data for every day for each point. However, due to the difficulties in getting the data from Meteocat only the rainy days were selected to be analysed. Rainy days were selected manually by searching the precipitation data of the network of automatic weather Stations (XEMA) inside the area of the study. This fact forced to focus only on the precipitation that reaches the ground and to leave the analysis of virga cases for later studies.

Here we have used the CAPPI third level, 2 km above sea level. We have selected it because is usually not affected by ground clutter and provide better reflectivity data than lower levels.

C. Rainfall regime analysis

The program to analyse the reflectivity data was designed by Powell et al. (2016). This code was done to study rainstorms in a tropical area with a S-band meteorological radar. In their study they analyse one level of the CAPPI reflectivity data and give a classification of 6 different rainfall type: Stratiform Rain, Convective Rain, Mixed, Iso Convective Fringe, Convective Core and Weak Echo.

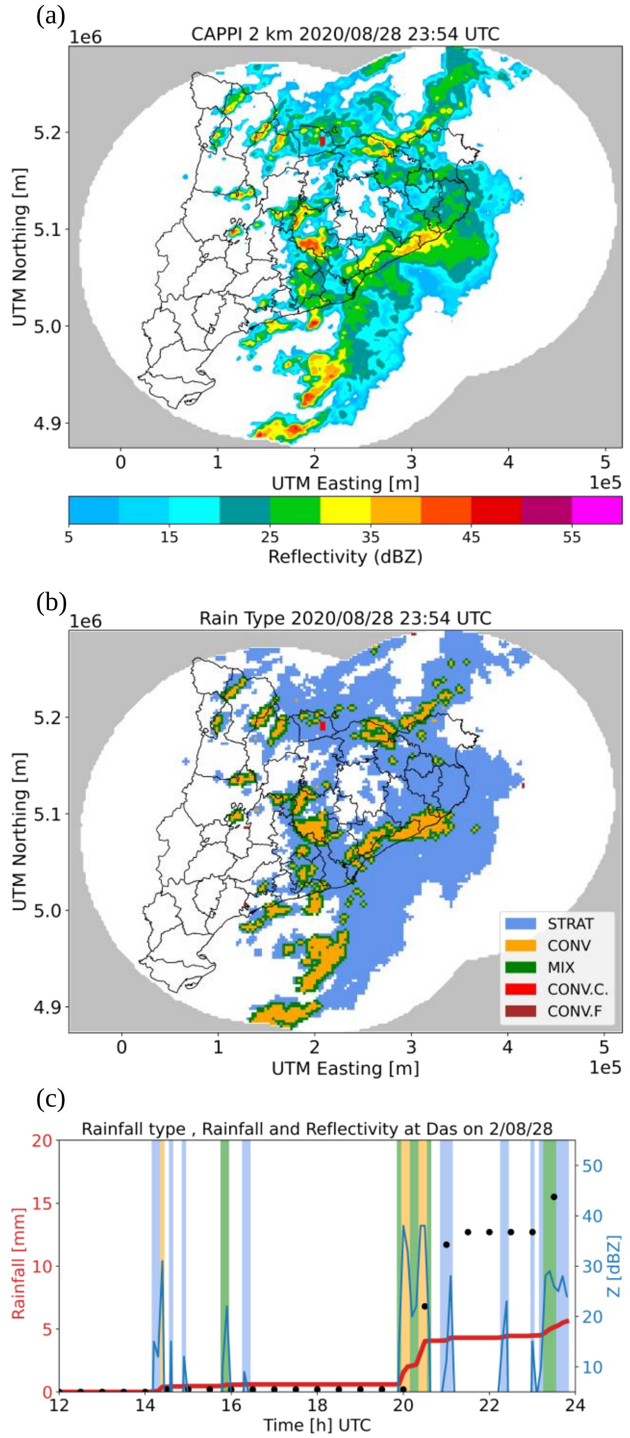

Figure 4. Reflectivity, Rainfall type, and Rainfall in Das for 2020/08/28 plots. [a], Reflectivity CAPPI 2 km 2020/08/28 23:54 UTC, Red point indicates Das location. [b] Rainfall type classification at 2020/08/28 23:54 UTC, Red point indicates Das location. [c], Das Rainfall rate evolution during 2020/08/28, reflectivity (blue line), accumulated rainfall calculated by the reflectivity (red line), coloured areas indicate the rainfall type (see in middle figure legend) and black points the accumulated rainfall from the rain gauge at of Das aerodrome.

This method is an improvement of previous schemes like defining a decreasing function around the highest reflectivity levels to determinate the Convective Region (Steiner et al., 1995). The current method evaluates the reflectivity value and the area of the precipitation to assess the regime of the rain. If the reflectivity is greater than a specific threshold and in a small area, it is considered a Convective Core or Convective Rain. If it has less reflectivity but has an extended area of rain, then it is considered Stratiform Rain. The precipitation area between the convective area and the stratiform rain is classified as Mixed Regime. The Iso Convective Fringe are the small precipitation areas which can turn to stratiform rain or to convective rain depending on their evolution. Finally, the program considers Weak Echo all reflectivity pixels that are below 5 dBZ. As the program is based on a tropical region and for an S-band radar the main parameters must be fixed to adapt the program to our data.

To be sure that the program works well we compared the rainfall type results with the underestimation of rainfall rate by a rain gauge. In this case we analyse the full rainfall of a day and we confirmed that the times of maximum rainfall rate of the rain gauge at Das (La Cerdanya) where the same ones the program the program classifies the rain as convective rain (**Figure 4**).

D. Main study Variables

The main variables used to obtain the results of the data are the following:

- **Rainfall type:** the rainfall type is the classification of the regime of rain: to simplify the analysis we consider only two rain types, Convective or Non convective.
- **Rainfall:** the amount in mm of water that fall in an area in a specific time period.
- **Rain-occurrence:** the number of events with rain.
- **Rainfall rate:** the intensity in mm/h of the rainfall.
- **Precipitation area:** number of pixels that have a reflectivity value higher than 5 dBZ.
- **Areal Precipitation:** According to the AMS (2021) "Precipitation in a specific area expressed as an average depth of liquid water over the area". It is expressed in mm.

All these variables are studied for the two regimes of rain, Convective and non-Convective, to explore differences between the general characteristics of the rain of the two areas.

E. Data Analyses and statistics

To perform all the analyses and the graphical representation of the data we have used Python programs. For the statistical analyses the two-tail Mann-Whitney Test and the two-tail Wilcoxon tests were used for the non-paired and paired data respectively. Differences were considered significant if P-values were lower than 0.05.

III. RESULTS

As mentioned above we focused on the analysis of the rain data of the summer months during the 2014-2020 period to search for different characteristics between the West and the East areas: irrigated and non-irrigated areas, respectively. We will analyse the reflectivity data, the diurnal cycle, the monthly summer distribution, the rainfall, and the total accumulated rainfall of the two areas.

A. Radar Reflectivity

When plotting the frequency distribution of the reflectivity of each point and the accumulated probability of the two areas (**Figure 5**), it is noticeable that the most common values are those lower than 15 dBZ and that the frequencies do not follow a normal distribution. Also, despite both areas seem to have a similar distribution, the P-Value of the Mann – Whitney test indicates that the two groups have a significant difference of the median values. That means that it could be a real difference between the two regions in the rainfall, but this should be considered carefully because not all events analysed are independent between them, since some of them may come from the same rain episode. For this reason, aggregated data per day or month will be used in the next sections.

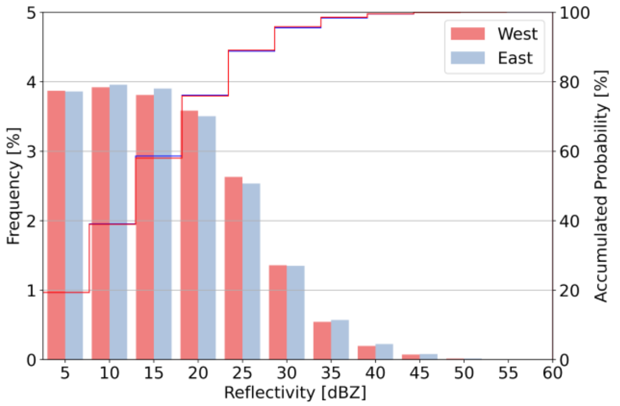

Figure 5: Frequency distribution (left y-axis) from radar reflectivity in the two areas West (red) and East (blue) and its accumulated probability (right y-axis). Period analysed: summer months from 2014 to 2020.

B. Precipitation overview

To evaluate the rainfall, a Z-R relationship equation (1) was use:

$$Z = a \cdot R^b \quad (1)$$

This equation gives us a value of a rainfall rate R (mm/h) from a reflectivity value Z (mm^6 m^{-3}). The parameters that are used are the Marshall – Palmer (a=200 and b=1.6) for the stratiform rain and Joss parameters (a=500 and b=1.5) for the convective rain (Fabry, 2015).

Using the rainfall rate, we calculated the parameters shown in **Table 1**. We corroborated that the area of study is a dry area with a mean of 4 days of rain, 16 mm of areal precipitation and 45% of Convective Rainfall per month during the summer. In addition, all the variables had a high dispersion, meaning that the precipitation phenomena vary a lot during the months and the years. Furthermore, there are no substantial differences in the number of rainy days and in the rainfall and the convective rainfall per month between the two areas. Moreover, we found that, in most cases, the rainy days coincide in both areas: there are only 5 days out of 157 days in the 2014 – 2020 period, in which it has only rained in one of the two areas.

C. Diurnal Cycle

In other to analyse the diurnal cycle of the rain, the day was divided in six parts of four hours each one.

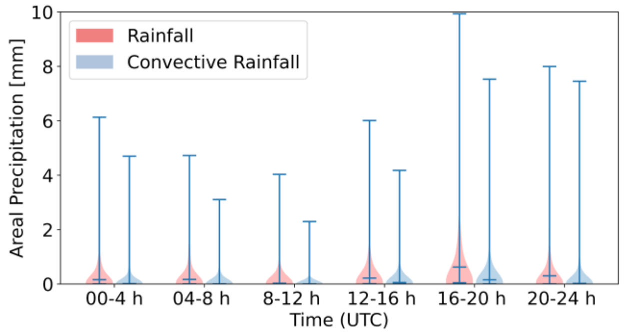

Figure 6. Diurnal distribution of areal precipitation [mm] violin plots for total rainfall (red) and convective rainfall (blue). Violins shows the extreme values and 25%, 50% and 75% percentiles with horizontal lines.

As shown in **Figure 6**, there is an increase of the rainfall and the convective rainfall in the last hours of the day, especially from 16:00 to 20:00. In fact, there is a significant statistical difference (P-Value less than 0.02, Mann-Whitney test) when comparing the 16-20 hours period vs all-morning periods.

Evaluating the diurnal distribution of the convective rainfall of both areas separately (**Figure 7**), we can see again an increase of the convective precipitation in the late afternoon hours, but that the two areas follow the same distribution.

	nº days with Rainfall greater than 1 mm		**Areal Precipitation [mm]**		**Rainfall Convective Fraction**	
	West [Days] ± σ	**East [Days] ± σ**	**West [mm] ± σ**	**East [mm] ± σ**	**West ± σ**	**East ± σ**
June	5 ± 3	6 ±2	20 ±12	22 ±11	0.4 ±0.1	0.4 ±0.1
July	4 ±2	4 ±2	15 ±9	15 ±11	0.5 ±0.1	0.5 ±0.1
August	3 ±1	3 ±2	13 ±5	12 ±5	0.5 ±0.2	0.5 ±0.2
Season monthly mean	4 ±1	4 ±1	16 ±4	16 ±4	0.5 ±0.1	0.5 ±0.1

Table 1. Monthly and season means and standard deviations of number of days with rainfall greater than 1 mm, total areal precipitation, and the fraction of convective rainfall.

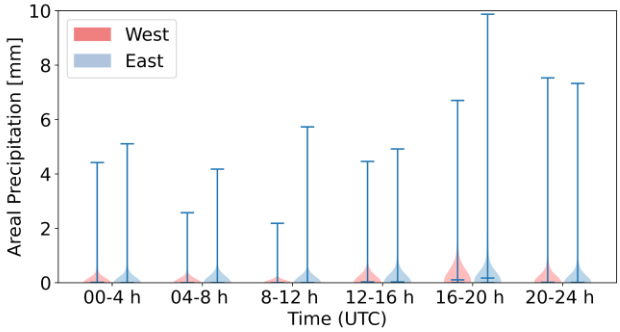

Figure 7. Diurnal distribution of areal convective precipitation [mm] violin plots for the West (red) and East (blue). Violin plots show the extreme values and 25%, 50% and 75% percentiles with horizontal lines.

D. Monthly summer distribution

We also analysed the monthly distribution of the rain during the summer months (June, July and August) in the two areas, West and East, for the years 2014 to 2020.

Figure 8 and **Figure 9** show the violin plots of the areal precipitation rainfall [mm], and the convective fraction of the total rainfall. Although differences between months are observed (June seems to have more total rainfall than August, and the fraction of rainfall seems to be higher in July) no significant differences were obtained between months and neither between irrigated (West) and non-irrigated (East) areas.

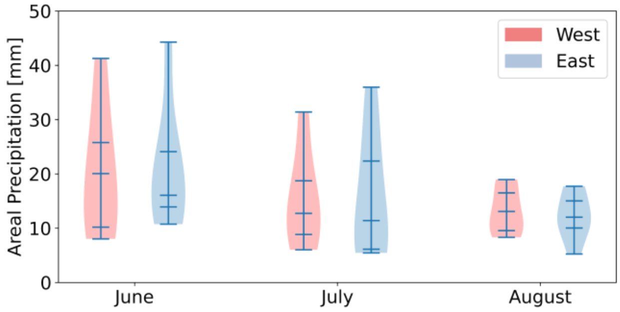

Figure 8. Summer month by areal precipitation violin plots, for West (red) and East (blue) areas. Violin plots show the extreme values and 25%, 50% and 75% percentiles with horizontal lines.

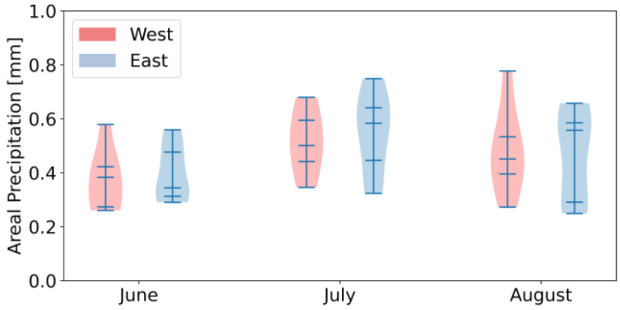

Figure 9. Convective rainfall fraction violin plots, for West (red) and East (blue) areas. Violin plots show the extreme values and 25%, 50% and 75% percentiles with horizontal lines.

Basically, the main limitation of these statistics is the reduced number of years analysed. There are only 7 points (years) per month, so there are not enough data to find statistically significant differences.

Again, in the plots it is possible to see the main characteristics of the whole area with a small rainfall during the summer month and a big variability between the years.

E. West – East Rainfall Distribution

In this section all rainy days are analysed to study the possible differences between the West and the East areas. The number of points of each violin plot is the maximum number of rainy days for each area. That means that only the days where there was no rain in the two areas are excluded. In total there are 150 days in the period of 2014-2020 which should be enough data to get significant results.

We first analysed the rainfall areal precipitation for the West and the East part and the Convective Rainfall Areal Precipitation (**Figure 10**). All violin plots show similar distributions in both areas and, in fact. there are no significant differences between them. In the West area there is a median of 1.9 mm per day, and the 25% and 75% quartiles are 1.3 mm and 4.0 mm, respectively. For the East part, the median is 2.3 mm per day and the 25% and 75% quartiles are 1.4 mm and 4.0 mm. Regarding to the areal convective precipitation, 50% of the rainy days have an areal convective rainfall of 0.2 mm and 2.0 mm in the West and 0.3 and 1.8 in the East, with a median of 0.8 mm and 0.9 mm respectively.

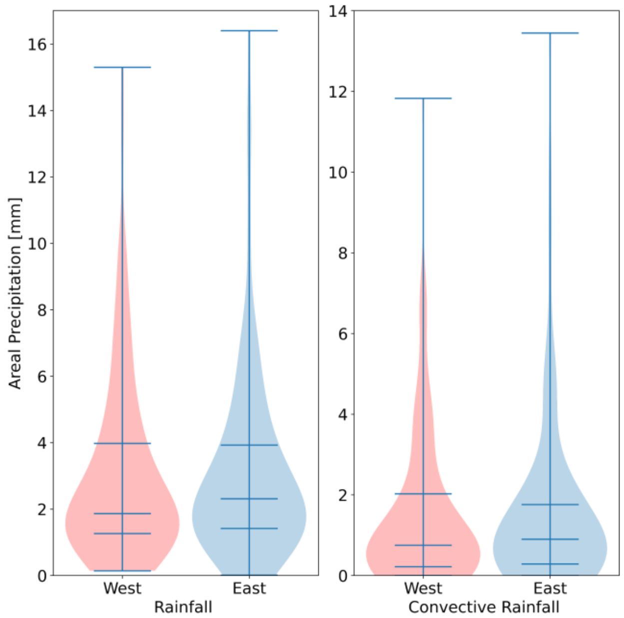

Figure 10. [Left] Areal precipitation [mm] of each rainy day. [Right] Convective areal precipitation [mm] of each rainy-day. West (red) and East (blue) areas. Violins plots show the extreme values and 25%, 50% and 75% percentiles with horizontal lines.

Then, with the aim to determine if there were differences in the area covered by convective rain between West vs East regions, accumulated area of convective rain during all day and the convective rain covered area divided by the total area of rain were calculated (**Figure 11**).

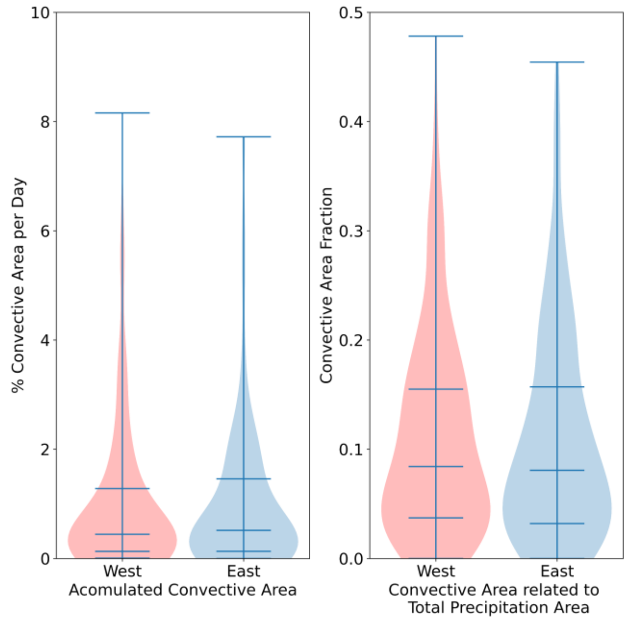

Figure 11. [Left] Percentage of accumulated convective area during the whole day violin plots. A value of 100 % would indicate that during the whole day the area has been covered by convective rain. [Right] Convective areal precipitation related to convective area. West (red) and East (blue) areas. Violin plots show the extreme values and 25%, 50% and 75% percentiles with horizontal lines.

The violin plots of **Figure 11** show that the 50% of days in the West have a total accumulated convective area between 0.3 % and 3.0 % with a median of 1.1%. In the East, 50 % of the days have a total accumulated area between 0.3 % and 3.5 % with a median of 1.2 %. This indicates that the convective rainfall is extended in small areas in each phenomenon, and since no significant differences are observed, the extension of the covered areas is similar in both regions.

In relation to the convective area fraction, the results do not present a statistical significance difference between both parts, with 50 % of the days with a fraction between 0.04 and 0.16 in the West and between 0.03 and 0.16 in the East.

The parameters analysed until now are related to the values of each aggregated area for each day, and we concluded that there are not significant differences between West and East during the summer days of the years 2014 - 2020.

Next we focused to study separetely each point of the grid, instead of grouping all the West points and all the East points together. In **Figure 12** the total connvective rainfall per year for each grid point is plotted.

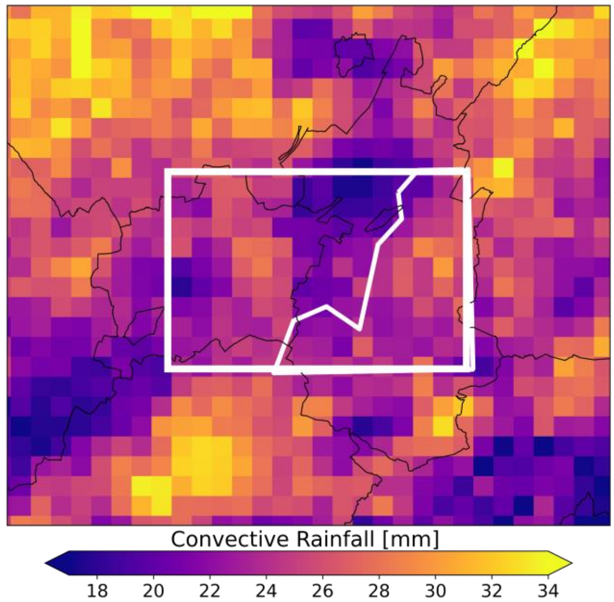

Figure 12. Year Average of Convective Rainfall [mm] for each point. White lines indicate the area of study and the division between the West and East parts. Black lines are the county limits of the zone of study.

Although the differences between the minimum and the maximum rainfall per grid-point are not big, we can observe zones with more convective rainfall than others. Thus, we evaluated if there were statistically significant differences of the accumulated total convective rain fall for each grid-point.

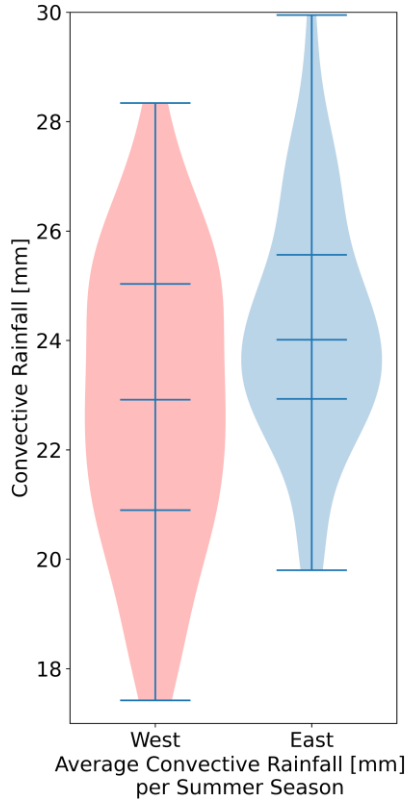

Figure 13. Distribution of Convective Rainfall per year of each pixel for the West and East areas. The data graphed is from the map of **Figure 12**. West (red) and East (blue) areas. Violins shows the extreme values and 25%, 50% and 75% percentiles with horizontal lines.

As shown in **Figure 13** there are important differences between the two areas in relation to the convective rainfall per year for grid-point (Mann-Whitney test has a P-value lower than 0.01). In the East area the distribution is nearly normal with a mean of 24 mm and 25% and 75% quartiles of 23 mm and 26 mm. The West distribution does not follow a strict normal distribution and has almost two maximums (**Figure 14**) with a mean of 23 mm and 25% and 75% quartiles of 21 mm and 25 mm.

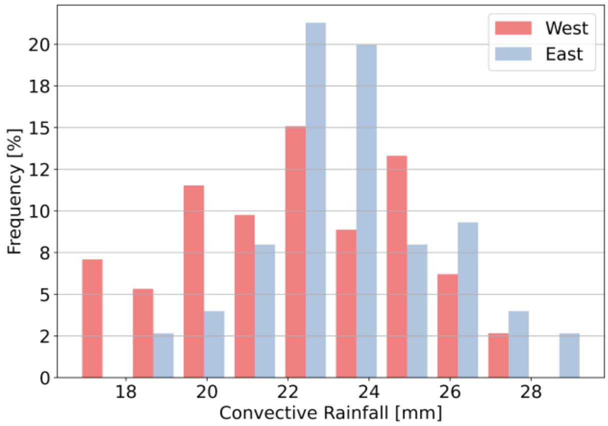

Figure 14. Frequency distribution of the average convective rainfall [mm] for each point of the two areas.

This result must be well interpreted, it does not mean that in one of the two areas rains more than in the other, it indicates how the rainfall episodes are distributed along the areas. We show the existence of a different distribution in each area; in the West area the distribution of the rain is less homogeneous, with a difference of the quartiles 25% and 75% of 5 mm, while in the East area the difference between quartiles 25% and 75% is only 3 mm.

IV. DISCUSSION

In this work we have studied and characterized the precipitation of two continuous areas, one irrigated and the other non-irrigated. The study has been done by analysing the reflectivity data and classifying the type of precipitation as convective or non-convective with the main objective to study if there are differences related to the precipitation between the two areas during the summer months. Since the rainy days were selected with the data form the meteorological stations of the area, one criticism to our work is that it is possible that not all the rainy days are accounted in the data, that would be the case if in the meteorological station did not rain.

The hypothesis of the existence of differences between the two areas is based on the presence of a strong gradient of surface temperatures between the two areas during the day. This difference could make a big influence on the boundary layer, the precipitation, and the general conditions of each area (McPherson, 2007).

First, when analysing the general characteristics of the area we observed that there is a lot of variability of rainy days, and rainfall, every year. That could be because both areas are affected equally by the general mesoscale meteorological phenomena that effect the region and change every year depending mostly on the synoptic conditions. But when searching for variations between the areas, we did not obtain significant differences related to the total rainfall of each part and neither for the total convective rainfall. Then it seems that the difference of surface temperatures does not affect the total rain of the data examined.

Previous studies which also analysed different characteristics of wet and dry surfaces, found that the presence of a low-level jet influences the afternoon rainfall differently in wet or dry areas: increasing the rainfall in the wet ones and decreasing it in the dry ones (Ford et al., 2015). The existence of a low-level jet does not seem to play a role in our area of study, since analysing the data making pairs of each rainy day (thus the same contour conditions) no differences of rainfall between wet and dry region where observed.

Regarding to the diurnal cycle, as we expected, there are significant differences between the convective rainfall hours. The convective rainfall increases in the late afternoon hours probably due to the increase of the surface temperature and the instability of the atmosphere. Other studies found differences regarding the afternoon rainfall in wet soils and dry lands (Taylor et al., 2012; Welty et al., 2020). But again, this does not seem to be our case since there are no differences in the rainy days between the two areas. Giving once more support to the conclusion that the rain in the area is mainly governed by the mesoscale phenomena during the summer months that affect the Northeast of Iberian Peninsula, and it is not influenced by the local conditions of the different irrigated and non-irrigated areas.

Interestingly, we observed significant differences between the accumulated rainfall distribution across the surface in both areas. The amount of rainfall is nearly the same in the two areas, but it is differently distributed in the terrain. Other studies focused on the impact that irrigation land has on the precipitation during heatwaves (Valmassoi et al., 2020) and found that the irrigation increases the boundary layer moisture, the CAPE and the precipitation, and decreases the level of free convection. This would agree with our finding that in the West part the convective rainfall is less homogenously distributed. But to explain this phenomenon and understand the causes, more studies should be done. For instance, the correlation between other parameters, like the temperature or the general advections of winds, should be studied, to determine if these differences come from the irrigation or are intrinsic differences of the area.

The effect of a channel in the local atmospheric climate is a very interesting and important aspect assess for future projects related with the construction of channels, swamps or other infrastructures that could change the surface characteristics. For example, the way that crop fields are irrigated may have an important effect to local climate change (Zou et al., 2012). In this direction the future demand of renewable energies could lead to extended areas covered with solar panels. These solar panels could change the albedo and the characteristics of the surface changing the local or even the global climate (Barron-Gafford et al., 2016; Hu et al., 2016; Lu et al., 2021).

For this reason, it is necessary to study and evaluate the possible consequences of all the land-surface changes that humans make in a specific area.

V. CONCLUSIONS

The summer months precipitation from 2014 to 2020 has been analysed with reflectivity radar data over a region of study, indicating the areas have an average of only 4 days of rain each summer month. The range of variability of this average along the year is very big indicating that the rainfall is governed by the general atmospheric conditions of the NE Iberian Peninsula.

The diurnal cycle studied is similar in the irrigated and non-irrigated areas and has a clear increase of the convective rainfall in the late afternoon hours.

There are no differences between the convective rainfall of both areas, irrigated and non-irrigated, with similar mm of convective rain per day and covering a similar terrain surface in the two areas.

The accumulated convective rainfall presents a more uniform area distribution in the East part than in the West part.

Future work will address other phenomena of the area, like the temperature, the virga or the wind fluxes to evaluate the effect of the irrigated parts in the region.

Acknowledgments

I would like to thank my tutor Dr. Joan Bech, for all the attention, the kindness, and the proximity despite the difficulties of the pandemic situation. To Francesc Roures and Enric Casellas for the help and advice in the start of the work, and to all the professors and classmates. Of course, a special dedication to my brother, my partner and of course my mum and finally, a very important mention to may late father Artur Polls which has helped me a lot despite not been here.

VI. REFERENCES

AMS. (2021). *Glossary of Meteorology*. GLOSSARY OF... https://glossary.ametsoc.org/wiki/Convective_precipitation

Barron-Gafford, G. A., Minor, R. L., Allen, N. A., Cronin, A. D., Brooks, A. E., & Pavao-Zuckerman, M. A. (2016). The Photovoltaic Heat Island Effect: Larger solar power plants increase local temperatures. *Scientific Reports*, *6*(1), 35070. https://doi.org/10.1038/srep35070

Bech, J., Vilaclara, E., Pineda, N., Rigo, T., Lorente, J., & Sempere, D. (2005). *ERAD 2004*. *2002*(2004), 416–420.

Boone, A., Best, M., Cuxart, J., Polcher, J., Quintana, P., Bellvert, J., Brooke, J., Canut-Rocafort, G., & Price, J. (2019). Land Surface Interactions with the Atmosphere over the Iberian Semi-Arid Environment (LIAISE). *GEWEX News*, *29*(1), 8–10.

Cuxart, J., Cunillera, J., Jiménez, M. A., Martínez, D., Molinos, F., & Palau, J. L. (2012). Study of Mesobeta Basin Flows by Remote Sensing. *Boundary-Layer Meteorology*, *143*(1), 143–158. https://doi.org/10.1007/s10546-011-9655-8

Drobinski, P., Ducrocq, V., Alpert, P., Anagnostou, E., Béranger, K., Borga, M., Braud, I., Chanzy, A., Davolio, S., Delrieu, G., Estournel, C., Filali Boubrahmi, N., Font, J., Grubišić, V., Gualdi, S., Homar, V., Ivančan-Picek, B., Kottmeier, C., Kotroni, V., … Wernli, H. (2014). HYMEX: A 10-year multidisciplinary program on the mediterranean water cycle. *Bulletin of the American Meteorological Society*, *95*(7), 1063–1082. https://doi.org/10.1175/BAMS-D-12-00242.1

Fabry, F. (2015). *Radar Meteorology: Principles and Practice*. Cambridge University Press. https://doi.org/DOI: 10.1017/CBO9781107707405

Ford, T. W., Rapp, A. D., & Quiring, S. M. (2015). Does afternoon precipitation occur preferentially over dry or wet soils in Oklahoma? *Journal of Hydrometeorology*, *16*(2), 874–888. https://doi.org/10.1175/JHM-D-14-0005.1

Houze, R. A. (1997). Stratiform Precipitation in Regions of Convection: A Meteorological Paradox? *Bulletin of the American Meteorological Society*, *78*(10), 2179–2196. https://doi.org/10.1175/1520-0477(1997)078<2179:SPIROC>2.0.CO;2

Hu, A., Levis, S., Meehl, G. A., Han, W., Washington, W. M., Oleson, K. W., van Ruijven, B. J., He, M., & Strand, W. G. (2016). Impact of solar panels on global climate. *Nature Climate Change*, *6*(3), 290–294. https://doi.org/10.1038/nclimate2843

Llasat, M. C. (2001). An objective classification of rainfall events on the basis of their convective features: Application to rainfall intensity in the Northeast of Spain. *International Journal of Climatology*, *21*(11), 1385–1400. https://doi.org/10.1002/joc.692

Lu, Z., Zhang, Q., Miller, P. A., Zhang, Q., Berntell, E., & Smith, B. (2021). Impacts of Large-Scale Sahara Solar Farms on Global Climate and Vegetation Cover. *Geophysical Research Letters*, *48*(2), e2020GL090789. https://doi.org/https://doi.org/10.1029/2020GL090789

McPherson, R. A. (2007). A review of vegetation—atmosphere interactions and their influences on mesoscale phenomena. *Progress in Physical Geography: Earth and Environment*, *31*(3), 261–285. https://doi.org/10.1177/0309133307079055

Powell, S. W., Houze, R. A., & Brodzik, S. R. (2016). Rainfall-type categorization of radar echoes using polar coordinate reflectivity data. *Journal of Atmospheric and Oceanic Technology*, *33*(3), 523–538. https://doi.org/10.1175/JTECH-D-15-0135.1

Rigo, T., Pineda, N., & Bech, J. (2008). Estudi i modelització del cicle de vida de les tempestes amb tècniques de teledetecció. In *Notes d'Estudi del Servei Meteorològic de Catalunya* (Vol. 72). http://static-m.meteo.cat/wordpressweb/wp-content/uploads/2014/11/18130754/Nota-Estudi-Tempestes.pdf

Roura, F. (2020). *Analysis of a first approximation to radar-based precipitation climatology over a highly contrasted land use region*.

SMC. (2021). El Clima de Catalunya. https://www.meteo.cat/wpweb/climatologia/el-clima-ahir/el-clima-de-catalunya/

Steiner, M., Houze, R. A., & Yuter, S. E. (1995). *Climatological Characterization of Three-Dimensional Storm Structure from Operational Radar and Rain Gauge Data*. 1978–2007. https://doi.org/10.1175/1520-0450(1995)034%3C1978:CCOTDS%3E2.0.CO;2

Taylor, C. M., de Jeu, R. A. M., Guichard, F., Harris, P. P., & Dorigo, W. A. (2012). Afternoon rain more likely over drier soils. *Nature*, *489*(7416), 423–426. https://doi.org/10.1038/nature11377

Thurai, M., Gatlin, P. N., & Bringi, V. N. (2016). Separating stratiform and convective rain types based on the drop size distribution characteristics using 2D video disdrometer data.

Atmospheric Research, *169*. https://doi.org/10.1016/j.atmosres.2015.04.011

Valmassoi, A., Dudhia, J., di Sabatino, S., & Pilla, F. (2020). Irrigation impact on precipitation during a heatwave event using WRF-ARW: The summer 2015 Po Valley case. *Atmospheric Research*, *241*(August 2019), 104951. https://doi.org/10.1016/j.atmosres.2020.104951

Welty, J., Stillman, S., Zeng, X., & Santanello, J. (2020). Increased Likelihood of Appreciable Afternoon Rainfall Over Wetter or Drier Soils Dependent Upon Atmospheric Dynamic Influence. *Geophysical Research Letters*, *47*(11), 1–9. https://doi.org/10.1029/2020GL087779

Zou, X., Li, Y. e., Gao, Q., & Wan, Y. (2012). How water saving irrigation contributes to climate change resilience-a case study of practices in China. *Mitigation and Adaptation Strategies for Global Change*, *17*(2), 111–132. https://doi.org/10.1007/s11027-011-9316-8

APPENDIX

List of variables and its values used in the algorithm in this work, program designed by Powell et al. (2016):

- truncZconvthers = 30
- dBZformaxconvradius = 40
- backgrndradius = 5
- maxConvRadus = 5
- weackechothres = 5
- shallowconvmin = 10
- minsize = 10
- startslope = 8
- maxsize = 10